

Short Communication

Molecular Analysis of Mutant and Wild-Type Tau Deposited in the Brain Affected by the FTDP-17 R406W Mutation

Tomohiro Miyasaka,^{*†}
Maho Morishima-Kawashima,<sup>* Rivka Ravid,[‡]
Peter Heutink,[§] John C. van Swieten,[¶]
Kazuo Nagashima,[†] and Yasuo Ihara^{*||}</sup>

From the Department of Neuropathology,^{*} Faculty of Medicine, University of Tokyo, Tokyo, Japan; the Laboratory of Molecular and Cellular Pathology,[†] School of Medicine, Hokkaido University, Sapporo, Japan; the Netherlands Brain Bank,[‡] Amsterdam, The Netherlands; the Departments of Clinical Genetics[§] and Neurology,[¶] Erasmus University, Rotterdam, The Netherlands; and Core Research for Evolutional Science and Technology (CREST),^{||} Japan Science and Technology Corporation (JST), Kawaguchi, Japan

Frontotemporal dementia and parkinsonism linked to chromosome 17 (FTDP-17) is a familial neurological disorder, characterized genetically by autosomal dominant inheritance, clinically by behavioral abnormalities and parkinsonism, and neuropathologically by tauopathy. Linkage analyses of affected families have led to identification of several exonic and intronic mutations in the tau gene. In this study, we analyzed molecular species of tau in the soluble and insoluble fractions of brain affected by the FTDP-17 R406W mutation. Protein chemical analysis and Western blotting using site-specific antibodies indicated that almost equal amounts of wild-type and mutant tau were present in the Sarkosyl-insoluble fraction of the R406W brain. Consistent with this, wild-type and mutant tau colocalized in neurofibrillary tangles in the frontal cortex and hippocampus of the R406W brain. In contrast to soluble R406W tau, which was less phosphorylated than soluble wild-type tau, the Sarkosyl-insoluble mutant tau was highly phosphorylated as well as the insoluble wild-type tau. (*Am J Pathol* 2001, 158:373–379)

Neurofibrillary tangles (NFTs), one of the hallmarks of Alzheimer's disease (AD), consist of bundles of unit fibrils called paired helical filaments (PHFs). Because the areas

forming NFTs match precisely the areas exhibiting neuronal loss, the formation of NFTs is considered to be involved in a pathway leading to neuronal death. This assumption has been substantiated by a recent discovery of mutations in the tau gene in families afflicted with frontotemporal dementia and parkinsonism linked to chromosome 17 (FTDP-17).^{1–3} This disease entity is characterized neuropathologically by extensive neuronal loss that is predominant in the anterior part of the cortex, basal ganglia, and midbrain, and by the formation of PHF or PHF-like fibrils in neurons of affected regions. Filamentous tau inclusions were observed also in glial cells, especially in oligodendrocytes, in the brains of some FTDP-17 families.⁴ So far, more than 20 exonic and intronic pathogenic mutations have been identified in the tau gene. Exonic mutations are localized within or close to the microtubule (MT)-binding domain, whereas intronic mutations are clustered in the 5'-splice site of exon 10. Most exonic mutations have been claimed to have slightly or significantly decreased ability to promote MT assembly.^{5,6} On the other hand, some of the exonic and all of the intronic mutations increase splicing-in of exon 10, which encodes the second repeat in the MT-binding domain.^{2,7} This causes an increase in the levels of the four-repeat tau, which has a greater ability to promote MT assembly.^{8,9}

One speculation about the pathogenic mechanism of FTDP-17 is that most exonic mutations may reduce the affinity of tau for MTs, leading to their destabilization, and the resultant cytosolic free tau becomes highly phosphorylated and aggregates into PHF-like fibrils, which may in turn exert neurotoxicity. In all intronic and some exonic mutations, four-repeat tau is selectively deposited in affected brains.^{6,9} However, this kind of information is not available for any of the exonic mutations; we do not know

Supported in part by a Research Grant for Longevity Sciences from the Ministry of Health and Welfare, Japan.

Accepted for publication October 26, 2000.

Address reprint requests to Yasuo Ihara, M.D., Department of Neuropathology, Faculty of Medicine, University of Tokyo, 7-3-1 Hongo, Bunkyo-ku, Tokyo 113-0033, Japan. E-mail: yihara@m.u-tokyo.ac.jp.

whether mutant tau is preferentially deposited in brains with exonic mutations. We have, therefore, analyzed the proportion of mutant to wild-type tau in the soluble and insoluble fractions of FTDP-17 brains with R406W mutation (numbered according to the 441-residue isoform). In addition, we have examined by immunofluorescence microscopy, using site-specific antibodies, whether the wild-type and mutant tau colocalize or whether either tau is predominant in NFTs. The R406W mutation also has an unusual characteristic, in that the mutant tau is very little phosphorylated on Ser-396 and -404 within transfected cells and the cell-free system.¹⁰⁻¹² Thus, we have investigated whether the mutant tau (if any in the Sarkosyl-insoluble fraction) is hyperphosphorylated, like the wild-type tau in PHFs in AD brains.

Materials and Methods

Subjects

Brain tissues from two R406W patients (Patient 1, 70 years old, and Patient 2, 71 years old)^{13,14} were obtained through a rapid autopsy program of the Netherlands Brain Bank (average postmortem delay, 6 hours). The two patients had received thorough clinical examination, and the severity of the dementia was estimated according to the Reisberg scale.¹⁵ At autopsy, the brain was removed and macroscopically examined, followed immediately by dissection of the various areas according to a protocol. The dissected blocks were either fixed in 10% formalin or kept at -80°C until use. The additional tissue sections were from a R406W patient in a different family, who has already been reported by Reed et al.¹⁶ AD brains were kindly provided by Dr. Dennis J. Selkoe.

Tissue Fractionation

Brain tissues were homogenized in Tris-saline (TS; 50 mmol/L Tris-HCl, 150 mmol/L NaCl, pH 7.6) containing a cocktail of protease inhibitors as described previously.¹⁷ The homogenates were centrifuged at 540,000 × *g* for 20 minutes, and the supernatants (TS-soluble fraction) were obtained. After precipitation of crude tau with 50% saturated ammonium sulfate, half the amount of crude tau was treated with 10 U/ml of *Escherichia coli* alkaline phosphatase (type III, Sigma, St. Louis, MO) at 67°C for 3 hours in 50 mmol/L Tris-HCl (pH 8.3) containing protease inhibitors. Sarkosyl-insoluble pellets were prepared from TS-insoluble pellets as described previously (Sarkosyl-insoluble fraction).¹⁷

Purification of PHF-Tau

The PHF-tau-rich fraction was prepared from TS-insoluble pellets according to the procedure developed by Greenberg and Davies.¹⁸ After sucrose density-gradient centrifugation, the 35%/50% interface containing PHF-like fibrils was carefully aspirated and pelleted by brief centrifugation. The pellet was solubilized with 6 mol/L guanidine hydrochloride (GuHCl) and carboxymethyl-

ated with iodoacetate after reduction. After clearing by brief centrifugation, crude PHF-tau was further purified on an Aquapore RP300 column (2.1 × 30 mm; Applied Biosystems, Foster City, CA) by reverse phase high-performance liquid chromatography (RP-HPLC; Model 1090M; Hewlett-Packard, Waldbronn, Germany). This was done using a linear gradient of 20 to 40% acetonitrile in 0.1% trifluoroacetic acid (TFA) for 20 minutes at a flow rate of 0.2 ml/minute. The fractions containing full-length PHF-tau were identified by silver staining and Western blotting. For further separation, pooled PHF-tau was rechromatographed on an Aquapore BU300 column (2.1 × 30 mm; Applied Biosystems) with a gradient of 24 to 36% acetonitrile in 0.1% TFA for 30 minutes at a flow rate of 0.2 ml/minute. Soluble tau was purified from the TS-soluble fraction as described previously.¹⁷ Recombinant wild-type or mutant tau was expressed in *E. coli* BL21(DE3) and purified as described previously.⁵

Proteolytic Digestion and Mass Spectrometry

After dephosphorylation, purified PHF-tau was digested in 100 mmol/L Tris-HCl (pH 9.0) with *Achromobacter lyticus* protease I (API) at an enzyme to substrate ratio of 1:100 at 37°C for 16 hours. The generated peptides were fractionated by RP-HPLC on a Superspher RP-Select B column (2 × 125 mm, Merck, Darmstadt, Germany) using a gradient of 0 to 48% acetonitrile in 0.1% TFA for 24 minutes at a flow rate of 0.2 ml/minute. Analysis of the peptides was performed by matrix-assisted laser desorption ionization time-of-flight mass spectrometry on Voyager-DERP (PerSeptive Biosystems, Framingham, MA) as described previously.¹⁹

Antibodies

Site-specific polyclonal antibodies against wild-type and mutant tau were raised against synthetic 14-mer peptides conjugated with KLH: SGDTSPRHLSNVSC (AR406) and SGDTSPWHLNSVSC (AW406). For Western blotting, the antisera (1 μl) were preabsorbed with 10 nmol counterpart-epitope peptide at 37°C for 30 minutes to warrant specificity and used at a dilution of 1:2000. For an immunofluorescence study, the site-specific antibodies were affinity-purified with each corresponding antigen peptide after preabsorption with a counterpart-epitope peptide. Phosphorylation-dependent tau antibodies used were: tau 1 (epitope; nonphosphoSer-199 and -202; Chemicon, Temecula, CA), AT8 (phosphoSer-202 and phosphoThr-205), AT100 (phosphoThr-212 and phosphoSer-214; Innogenetics, Zwijndrecht, Belgium), M4 (phosphoThr-235), C5 (phosphoSer-396),²⁰ PHF1 (phosphoSer-396 and -404),²¹ and polyclonal AP422 (phosphoSer-422).²²

Western Blotting

Western blotting was performed as described previously.²³ Bound antibodies were detected by enhanced chemiluminescence (ECL; Amersham, Buckingham, UK).

Semiquantitative Western blotting was performed by several exposures of the ECL film to equalize the signal intensity toward the same amount of authentic recombinant wild-type and mutant tau. ECL bands of interest were quantified with a model GS-700 imaging densitometer on Molecular Analyst Software (Bio-Rad Laboratories, Hercules, CA). When required, dephosphorylation of tau was performed on the membrane, because the phosphorylation was found to affect immunoreactivities for AR406 and AW406 (data not shown).

Reverse Transcription-Polymerase Chain Reaction (RT-PCR)

Total RNA was purified from each brain tissue using an SV total RNA isolation system (Promega, Madison, WI). After reverse transcription primed by random hexamers, the cDNA was amplified with the following primer sets: 5'-AATATCACCCACGTCCTGGCGGAGGAAAT-3' for sense and 5'-ACAAACCCTGCTTGCCATGGAGGCAGACA-3' for antisense. Each PCR cycle consisted of 30 seconds at 94°C, 1 minute at 65°C, and 1 minute at 72°C. The PCR products were digested with *MspI* and *EcoT14I* to distinguish between wild-type and R406W cDNAs. After separation on a 6% acrylamide gel, the bands that visualized with an SYBR Green dye (Molecular Probes, Eugene, OR) were quantified with a Fluorolmager (Molecular Dynamics, Sunnyvale, CA).

Immunofluorescence Microscopy

Paraffin-embedded tissue sections were deparaffinized and dipped in formic acid for 4 minutes to enhance the staining for NFTs.²⁴ The sections were then pretreated with alkaline phosphatase before staining with 10 μ g/ml of affinity-purified AR406 and AW406 (see above). Bound antibodies were visualized using the avidin-biotin method (Vectastain Elite, Vector Laboratories, Burlingame, CA) with 3,3'-diaminobenzidine as a substrate. For immunofluorescence, purified AR406 and AW406 were labeled with Alexa 488 and Alexa 568 (Alexa Fluor 488 or 568 Protein labeling kit, Molecular Probes), respectively, according to the manufacturer's instructions, and used at a concentration of 20 μ g/ml. Lipofuscin autofluorescence was blocked by treating sections with 0.1% Sudan black B (Merck) in 70% ethanol for 10 minutes at room temperature.²⁵ Specimens were observed under a Zeiss Axioskop microscope (Carl Zeiss Inc., Thornwood, NY) and analyzed using a Bio-Rad laser scanning confocal imaging system (Microradiance R2000/AG-2) equipped with the Lasersharpp2000 software (Bio-Rad Laboratories).

Results

Site-Specific Antibodies Distinguished between Wild-Type and Mutant Tau in R406W Brain

To distinguish between wild-type and mutant tau in the fractions of R406W brain, we raised paired antibodies

that specifically recognize either wild-type or mutant tau. After preabsorption with the counterpart-epitope peptide, AR406 and AW406 reacted exclusively with R406R (wild-type) and R406W tau (mutant tau), respectively (Figure 1A). Using these site-specific antibodies, we examined tau in the TS-soluble and Sarkosyl-insoluble fractions of R406W brains. Both AR406 and AW406 labeled to a similar extent PHF-tau migrating at 60–70 kd and a smear²³ on a blot of Sarkosyl-insoluble fraction prepared from frontal cortices, temporal cortex, and hippocampus (Figure 1B). No specific labeling was found in the fraction from cerebella, which are usually free from NFTs. In contrast, as expected, only AR406 but not AW406 labeled PHF-tau and a smear in the Sarkosyl-insoluble fraction of an AD brain. Western blotting also showed that similar levels of wild-type and R406W tau were present in the TS-soluble fraction of frontal cortices and cerebella of R406W brains, when the signal intensities of the antibodies were normalized using authentic recombinant tau (see Materials and Methods) (Figure 1C). Consistent with this finding, quantitative RT-PCR showed no significant difference between the mRNA levels for wild-type and mutant tau in R406W brains (data not shown).

Both Wild-Type and Mutant Tau Were Equally Incorporated into PHF-Tau in R406W Brain

Because quantification by Western blotting left some ambiguities, we sought to determine the proportion of wild-type tau to R406W tau in PHF-tau by protein chemical analysis. When the HPLC profiles of API digests were compared, the most remarkable difference between the authentic recombinant wild-type and R406W tau was a shift of the late-eluting peak in the latter from 22.3 to 23.3 minutes (peaks 3 and 4 in Figure 1D, respectively). These peaks contained the carboxy-terminal API peptides (residues 396–438; see Figure 1E) generated from wild-type and R406W tau, respectively.¹⁷ This indicates that the substitution of a hydrophilic amino acid, Arg, to a hydrophobic aromatic amino acid, Trp, causes a retarded elution of this particular peptide.

PHF-tau purified from frontal cortices of the R406W brain (Patient 2) was subjected to API digestion after dephosphorylation. The HPLC profile of the API digest contained two separate late-eluting peaks (peaks 1 and 2 in Figure 1D), the elution positions of which corresponded exactly to those of the carboxy-terminal peptides from wild-type and R406W tau, respectively (peaks 3 and 4 in Figure 1D). The presence of the wild-type and mutant carboxy-terminal peptides in peaks 1 and 2, respectively, was further confirmed by mass spectrometry (Figure 1E). The similar heights of peaks 1 and 2 indicate that almost equal amounts of wild-type and R406W tau are incorporated into Sarkosyl-insoluble PHF-tau. One may argue that Trp has a large UV absorbance even at 215 nm and the amount of mutant peptide may be overestimated. Furthermore, the recovery yield might differ between the wild-type and mutant peptides. However, the peptide maps constructed from equal amounts (2 μ g for each) of recombinant wild-type and R406W tau

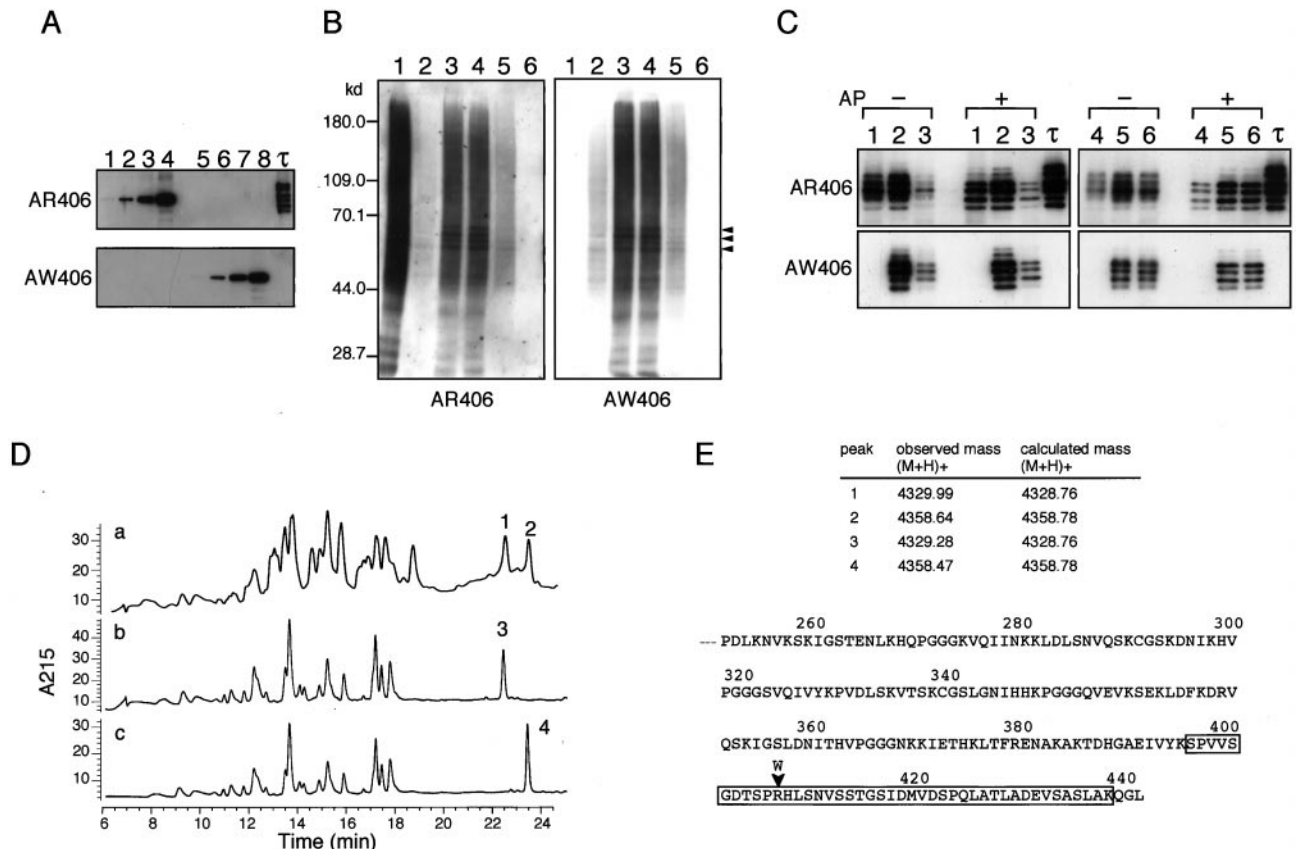


Figure 1. Western blots of TS-soluble and Sarkosyl-insoluble fractions of R406W brains and protein chemical analysis of PHF-tau purified from R406W brains. **A:** Specificities of AR406 and AW406 confirmed by Western blotting of recombinant wild-type (lanes 1–4) and R406W tau (lanes 5–8) as authentic antigens. Lanes 1 and 5, 0.8 ng; lanes 2 and 6, 4 ng; lanes 3 and 7, 20 ng; lanes 4 and 8, 100 ng; and τ (rightmost lane), six isoforms of recombinant tau. **B:** Sarkosyl-insoluble fractions prepared from frontal cortices of an AD patient (lane 1), R406W Patient 1 (lane 2), and Patient 2 (lane 3), temporal cortex of Patient 2 (lane 4), hippocampus of Patient 2 (lane 5) and cerebellum of Patient 2 (lane 6) were subjected to semiquantitative Western blotting with AR406 and AW406. PHF-tau (arrowheads) and a smear were labeled in specimens from various cortices of an AD and R406W brains, but not in those from cerebellum. In our hands, the 64-kD band of PHF-tau are usually resolved into closely spaced two bands. All samples corresponded to preparations from 0.5 mg wet weight tissue, except for a sample from Patient 1, which was from 2.5 mg wet weight tissue. **C:** TS-soluble fractions were prepared from frontal cortices (lanes 1–3) and cerebella (lanes 4–6) of an AD patient (lanes 1 and 4), R406W Patient 1 (lanes 2 and 5), and Patient 2 (lanes 3 and 6). Before or after dephosphorylation (AP), proteins equivalent to that contained in 1.0 mg tissue were subjected to semiquantitative Western blotting with AR406 and AW406. Note that wild-type tau but not mutant tau in the frontal cortex and cerebellum of R406W brains exhibited a slight but obvious mobility shift after dephosphorylation. Upper two bands in AP+ lanes probably come from indiscernible phosphorylated counterparts with slower mobility. **D:** The PHF-tau purified from R406W brains (a) and authentic recombinant wild-type (b) and R406W tau (c) were digested with API, and the produced peptides were separated on a Select B column as described in Materials and Methods. Note that the elution positions of peaks 1 and 2 (a) exactly correspond to those of peaks 3 (b) and 4 (c), generated from wild-type and mutant tau, respectively. **E:** The peptides in peaks 1–4 in D were subjected to matrix-assisted laser desorption ionization time-of-flight mass spectrometry. The amino acid sequence of the carboxy half of human tau is shown. The mutation is indicated by arrowhead, and the carboxy-terminal peptide (residues 396–438) is boxed.

showed equivalent peak areas for the carboxy-terminal fragments (data not shown), an observation that supports the above conclusion.

Wild-Type and Mutant Tau Colocalized in NFTs in R406W Brain

We next immunostained the tissue sections from various regions of R406W brains using the site-specific antibodies (Figure 2). There were a greater number of NFTs in the sections from Patient 2 than in those from Patient 1, which is consistent with the result of Western blotting (see Figure 1B). AR406 and AW406 labeled, to a similar extent, innumerable intracellular NFTs in neuronal perikarya, but not extracellular NFTs. This contrasted with robust labeling of extracellular NFTs with a monoclonal antibody to residues 368–386 (data not shown). Presumably, the carboxy-terminal portion of extracellular NFTs is cleaved

up to the locations of the epitopes for AR406 and AW406.²⁶ Large flame-shaped or globose NFTs and fine neuropil threads were abundant in layers II, III, and V in the frontal and temporal cortices (Figure 2, A and B, and data not shown). This laminar distribution was less distinct as compared with that seen in AD brain. Notably, many NFTs were observed in the dentate gyrus, which is barely affected by AD.

Although there were some variabilities in AR406 and AW406 signal intensities, the two signals always colocalized in all of the NFTs and neuropil threads examined in frontal cortex, hippocampus CA1, and dentate gyrus (Figure 2 and data not shown). Very few NFTs that were labeled similarly by both antibodies were found in the occipital cortex, the region least affected in FTDP-17 (data not shown). Similar immunofluorescence findings were obtained in another R406W brain from the American family (Figure 2, I and J).¹⁶ Under the same conditions, AW406 revealed no NFTs in AD

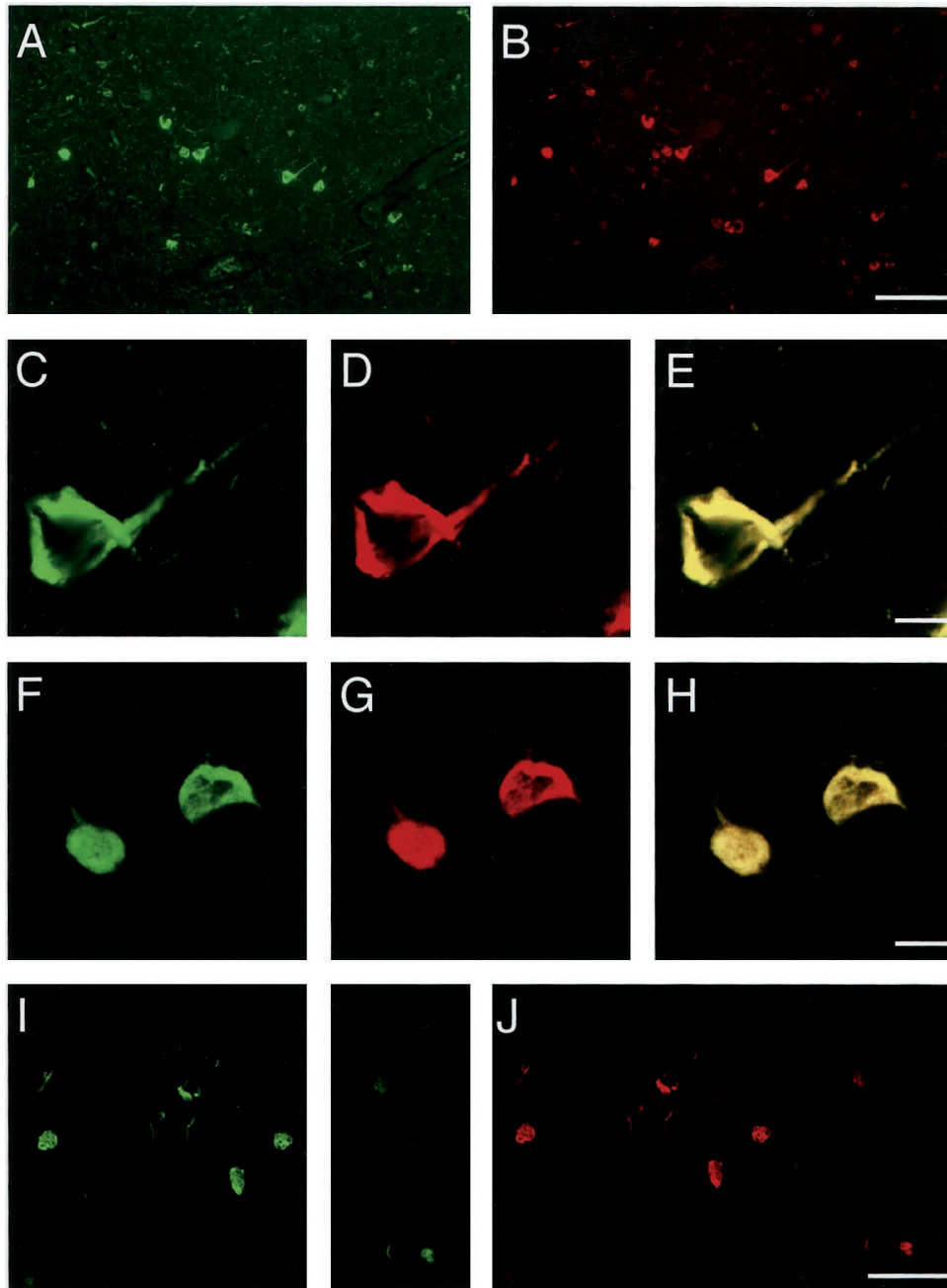


Figure 2. Double-labeled NFTs in R406W brains. Tissue sections from the frontal cortex and hippocampal region of R406W brain from the Dutch (**A-H**) and American families (**I and J**)¹⁶ were immunostained with Alexa 488-conjugated AR406 (green for wild-type tau) and Alexa 568-conjugated AW406 (red for mutant tau), as described in Materials and Methods. NFTs were labeled with both antibodies to a similar extent, indicating that wild-type and mutant tau coexist in NFTs in R406W brains. **C-J**: Confocal images of NFTs in the frontal cortex (**C-E**) and dentate gyrus (**F-H**) of Patient 2 from the Dutch family, and in the subiculum (**I and J**) of a patient from the American family.¹⁶ **E** and **H** represent merged views of **C** and **D** and of **F** and **G**, respectively. Scale bars, 100 μm (**A, B, I, and J**) and 10 μm (**C-H**).

brains (data not shown). These observations, together with the above biochemical result, indicate that wild-type and mutant tau are deposited at an equal proportion in any given affected neuron in R406W brain.

R406W Tau Is Aberrantly Hyperphosphorylated in PHF-Tau

Although R406W tau is very little phosphorylated on Ser-396 and -404 in transfected cells,¹⁰⁻¹² it remains un-

clear whether R406W tau in NFTs in the affected brain is less phosphorylated. In fact, abundant NFTs in R406W brain were intensely labeled with C5 and PHF1 (data not shown). Taken together, one might reasonably speculate that wild-type tau rather than mutant tau is preferentially phosphorylated in NFTs in the R406W brain. To assess the phosphorylation of R406W tau *in vivo*, pooled PHF-tau was rechromatographed with a shallow gradient to obtain a better separation of wild-type and mutant tau. Western blotting using AR406 and AW406 showed that early-

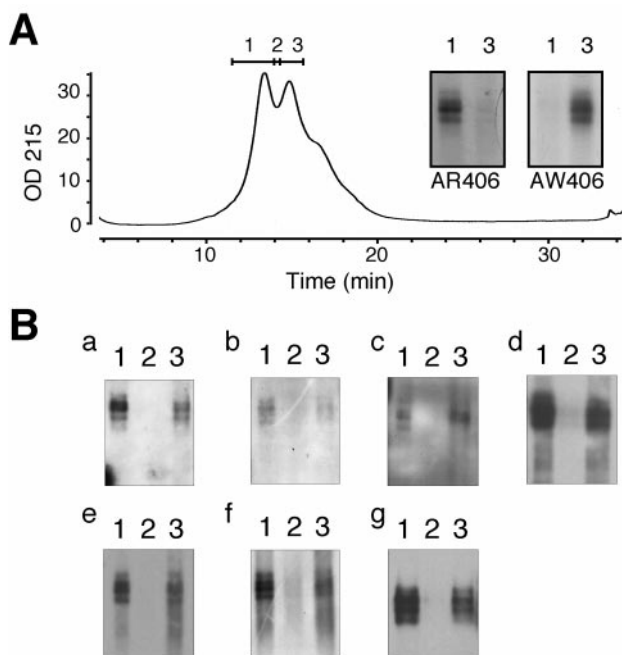


Figure 3. Hyperphosphorylation of R406W tau in PHF-tau. Purified PHF-tau was rechromatographed on an Aquapore BU300 column, with a shallow gradient of acetonitrile (A). Western blotting with AR406 and AW406 showed substantial separation between wild-type and R406W tau (inset, A). B: Each of fractions 1–3 was subjected to Western blotting with AT8 (a), AT100 (b), M4 (c), C5 (d), PHF1 (e), and AP422 (f) to evaluate the extent of phosphorylation of wild-type (fraction 1) and R406W tau (fraction 3). Western blotting using tau 1 after dephosphorylation (g) represents the amounts of all tau isoforms in each fraction.

eluting and late-eluting peaks consist largely of wild-type and R406W tau, respectively (inset in Figure 3A). A rough estimate of tau amounts present in each fraction can be made by the labeling with tau 1 after dephosphorylation (Figure 3B, g). PHF-tau in each peak was labeled intensely with C5 and PHF1, indicating that Ser-396 and –404 of both mutant and wild-type tau are highly phosphorylated in the PHF-tau from R406W brains (Figure 3B, d and e). Similar results were obtained using other phosphorylation-dependent antibodies including AT8, AT100, M4, and APP422 (Figure 3B).

In contrast, in the TS-soluble fraction, mutant tau appeared to be less extensively phosphorylated than wild-type tau, which was shown by the absence of mobility shift of the AW406-immunoreactive bands as compared with an obvious shift of AR406-reactive bands after dephosphorylation (Figure 2C).

Discussion

The present study has shown that the PHF-tau in R406W brains consists of wild-type and mutant tau at a ratio of approximately 1:1 (Figure 1, B and D). This agrees with the observation that levels of cytosolic mutant tau were not decreased compared with those of wild-type tau in the affected brain regions (Figure 1C). This may indicate that the mutant tau is not preferentially aggregated in the R406W brain. This assumption is supported by the absence of significant difference in the numbers of AR406-

and AW406-immunoreactive NFTs and neuropil threads even in less affected areas. Colocalization of wild-type and mutant tau in a given NFT raises the possibility that both species of tau compose heteropolymers in the process of NFT formation. The heterodimer rather than homodimer would be preferentially formed, and become a building block of the PHF-like fibril.

In R406W brains, the mutant tau incorporated into PHF-tau was aberrantly phosphorylated, similar to wild-type tau, whereas the mutant tau in the TS-soluble fraction was much less phosphorylated than wild-type tau (Figure 1C). The latter observation is consistent with the previous observations on R406W tau-transfected cells.^{10–12} Less phosphorylation of the mutant tau on Ser-396 and –404 may be due to a restriction imposed by Arg-to-Trp substitution. When the MT-binding domain of the cytosolic mutant tau is occupied by tubulin, a large residue (Trp) nearby may cause a significant restriction to the accessibility of protein kinases to these sites. Thus, a lesser extent of phosphorylation of the cytosolic mutant tau (see Figure 1C) may reflect the presence of abundant tubulin or MTs and resultant tau-tubulin interaction.

A large discrepancy in the extent of phosphorylation of R406W tau in the TS-soluble versus the Sarkosyl-insoluble fraction is of particular interest. The cytosolic mutant tau is resistant to phosphorylation on Ser-396 and –404, but when the disease process proceeds, the same sites become highly phosphorylated. Presumably, the process of deposition involves a large conformational change on the carboxy terminal to the MT-binding domain of mutant tau. When neurons undergo degeneration, MTs are rapidly lost, and their loss may result in an unfolded conformation in the MT-binding domain and adjacent regions of the mutant tau, which in turn enhances the phosphorylation of mutant tau on Ser-396 and –404 to an extent similar to that found in wild-type tau. At the same time, the absence of tubulin facilitates tau-tau interaction in the MT-binding domain to form fibrils. Thus, hyperphosphorylation of the mutant tau may reflect a loss of MTs from its surrounding.

Acknowledgments

We thank Dr. L. Reed for providing tissue sections from her R406W patient, Dr. M. Goedert for providing tau cDNA constructs, Drs. S. Greenberg and P. Davies for providing PHF1, and Drs. K. Takio and A. Watanabe for their help in protein chemical analysis.

References

1. Poorkaj P, Bird TD, Wijsman E, Nemens E, Garruto RM, Anderson L, Andreadis A, Wiederholt WC, Raskind M, Schellenberg GD: Tau is a candidate gene for chromosome 17 frontotemporal dementia. *Ann Neurol* 1998, 43:815–825
2. Hutton M, Lendon CL, Rizzu P, Baker M, Froelich S, Houlden H, Pickering-Brown S, Chakraverty S, Isaacs A, Grover A, Hackett J, Adamson J, Lincoln S, Dickson D, Davies P, Petersen RC, Stevens M, de Graaff E, Wauters E, van Baren J, Hillebrand M, Joosse M, Kwon JM, Nowotny P, Che LK, Norton J, Morris JC, Reed LA, Trojanowsky JQ, Basun H, Lannfelt L, Neystat M, Fahn S, Dark F, Tannenberg T, Dodd PR, Hayward N, Kwok JBJ, Schofield PR, Andreadis A, Snow-

- den J, Craufurd D, Neary D, Owen F, Oostra BA, Hardy J, Goate A, van Swieten J, Mann D, Lynch T, Heutink P: Association of missense and 5'-splice-site mutations in tau with the inherited dementia FTDP-17. *Nature* 1998, 393:702-705
3. Spillantini MG, Murrell JR, Goedert M, Farlow MR, Klug A, Ghetti B: Mutation in the tau gene in familial multiple system tauopathy with presenile dementia. *Proc Natl Acad Sci USA* 1998, 95:7737-7741
 4. Hutink P: Untangling tau-related dementia. *Hum Mol Genet* 2000, 12:979-986
 5. Hasegawa M, Smith MJ, Goedert M: Tau proteins with FTDP-17 mutations have a reduced ability to promote microtubule assembly. *FEBS Lett* 1998, 437:207-210
 6. Hong M, Zhukareva V, Vogelsberg-Ragaglia V, Wszolek Z, Reed L, Miller BI, Geschwind DH, Bird TD, McKeel D, Goate A, Morris JC, Wilhelmsen KC, Schellenberg GD, Trojanowski JQ, Lee VM: Mutation-specific functional impairments in distinct tau isoforms of hereditary FTDP-17. *Science* 1998, 282:1914-1917
 7. D'Souza I, Poorkaj P, Hong M, Nochlin D, Lee VM, Bird TD, Schellenberg GD: Missense and silent tau gene mutations cause frontotemporal dementia with parkinsonism-chromosome 17 type, by affecting multiple alternative RNA splicing regulatory elements. *Proc Natl Acad Sci USA* 1999, 96:5598-5603
 8. Goedert M, Jakes R: Expression of separate isoforms of human tau protein: correlation with the tau pattern in brain and effects on tubulin polymerization. *EMBO J* 1990, 9:4225-4230
 9. Spillantini MG, Goedert M, Crowther RA, Murrell JR, Farlow MR, Ghetti B: Familial multiple system tauopathy with presenile dementia: a disease with abundant neuronal and glial tau filaments. *Proc Natl Acad Sci USA* 1997, 94:4113-4118
 10. Dayanandan R, van Slegtenhorst M, Mack TG, Ko L, Yen SH, Leroy K, Brion JP, Anderton BH, Hutton M, Lovestone S: Mutations in tau reduce its microtubule binding properties in intact cells and affect its phosphorylation. *FEBS Lett* 1999, 446:228-232
 11. Matsumura N, Yamazaki T, Ihara Y: Stable expression in Chinese hamster ovary cells of mutated tau genes causing frontotemporal dementia and parkinsonism linked to chromosome 17 (FTDP-17). *Am J Pathol* 1999, 154:1649-1656
 12. Péres M, Lim F, Arresate M, Avila J: The FTDP-17-linked mutation R406W abolishes the interaction of phosphorylated tau with microtubules. *J Neurochem* 2000, 74:2583-2589
 13. van Swieten JC, Stevens M, Rosso SM, Rizzu P, Joosse M, de Koning I, Kamphorst W, Ravid R, Spillantini MG, Niermeijer MF, Heutink P: Phenotypic variation in hereditary frontotemporal dementia with tau mutations. *Ann Neurol* 1999, 46:617-626
 14. Spillantini MG, Crowther RA, Kamphorst W, Heutink P, van Swieten JC: Tau pathology in two Dutch families with mutations in the microtubule-binding region of tau. *Am J Pathol* 1998, 153:1359-1363
 15. Reisberg B, Ferris SH, de Leon MJ, Crook T: The Global Deterioration Scale for assessment of primary degenerative dementia. *Am J Psychiat* 1982, 139:1136-1139
 16. Reed LA, Schmidt ML, Wszolek ZK, Balin BJ, Soontornniyomkij V, Lee VM, Trojanowski JQ, Schelper RL: The neuropathology of a chromosome 17-linked autosomal dominant parkinsonism and dementia ("pallido-ponto-nigral degeneration"). *J Neuropathol Exp Neurol* 1998, 57:588-601
 17. Hasegawa M, Morishima-Kawashima M, Takio K, Suzuki M, Titani K, Ihara Y: Protein sequence and mass spectrometric analyses of tau in the Alzheimer's disease brain. *J Biol Chem* 1992, 267:17047-17054
 18. Greenberg SG, Davies P: A preparation of Alzheimer paired helical filaments that displays distinct tau proteins by polyacrylamide gel electrophoresis. *Proc Natl Acad Sci USA* 1990, 87:5827-5831
 19. Watanabe A, Takio K, Ihara Y: Deamidation and isoaspartate formation in smeared tau in paired helical filaments. Unusual properties of the microtubule-binding domain of tau. *J Biol Chem* 1999, 274:7368-7378
 20. Hasegawa M, Watanabe A, Takio K, Suzuki M, Arai T, Titani K, Ihara Y: Characterization of two distinct monoclonal antibodies to paired helical filaments: further evidence for fetal-type phosphorylation of the tau in paired helical filaments. *J Neurochem* 1993, 60:2068-2077
 21. Otvos L Jr, Feiner L, Lang E, Szendrei GI, Goedert M, Lee VM: Monoclonal antibody PHF-1 recognizes tau protein phosphorylated at serine residues 396 and 404. *J Neurosci Res* 1994, 39:669-673
 22. Morishima-Kawashima M, Hasegawa M, Takio K, Suzuki M, Yoshida H, Titani K, Ihara Y: Proline-directed and non-proline-directed phosphorylation of PHF-tau. *J Biol Chem* 1995, 270:823-829
 23. Morishima-Kawashima M, Hasegawa M, Takio K, Suzuki M, Titani K, Ihara Y: Ubiquitin is conjugated with amino-terminally processed tau in paired helical filaments. *Neuron* 1993, 10:1151-1160
 24. Kitamoto T, Ogomori K, Tateishi J, Prusiner SB: Formic acid pretreatment enhances immunostaining of cerebral and systemic amyloids. *Lab Invest* 1987, 57:230-236
 25. Schnell SA, Staines WA, Wessendorf MW: Reduction of lipofuscin-like autofluorescence in fluorescently labeled tissue. *J Histochem Cytochem* 1999, 47:719-730
 26. Endoh R, Ogawara M, Iwatsubo T, Nakano I, Mori H: Lack of the carboxyl terminal sequence of tau in ghost tangles of Alzheimer's disease. *Brain Res* 1993, 601:164-172